

# Superstructure and Mechanical Properties of Nylon 66 Microfiber Prepared by Carbon Dioxide Laser-Thinning Method

Akihiro Suzuki, Toshinori Hasegawa

Interdisciplinary Graduate School of Medicine and Engineering, University of Yamanashi, Takeda-4, Kofu 400-8511, Japan

Received 6 January 2005; accepted 17 April 2005

DOI 10.1002/app.22561

Published online in Wiley InterScience (www.interscience.wiley.com).

**ABSTRACT:** Nylon 66 microfibers were obtained by a carbon dioxide (CO<sub>2</sub>) laser-thinning method. A laser-thinning apparatus used to continuously prepare microfibers consisted of spools supplying and winding the fibers, a continuous-wave CO<sub>2</sub>-laser emitter, a system supplying the fibers, and a traverse. The diameter of the microfibers decreased as the winding speed increased, and the birefringence increased as the winding speed increased. When microfibers, obtained through the laser irradiation (at a power density of 8.0 W cm<sup>-2</sup>) of the original fiber supplied at 0.23 m min<sup>-1</sup>, were wound at 2000 m min<sup>-1</sup>, they had a diameter of 2.8 μm and a birefringence of 46 × 10<sup>-3</sup>. The draw ratio calculated from the supplying and winding speeds was 8696×. Scanning electron microscopy showed that the microfibers obtained with the laser-thinning appa-

ratus had smooth surfaces not roughened by laser ablation that were uniform in diameter. To study the conformational transition with winding speed, the changes in *trans* band at 936 cm<sup>-1</sup> and *gauche* band at 1136 cm<sup>-1</sup> were measured with a Fourier transform infrared microscope. The *trans* band increased as the winding speed increased, and the *gauche* band decreased. Young's modulus and tensile strength increased with increasing winding speed. The microfiber, which was obtained at a winding speed of 2000 m min<sup>-1</sup>, had a Young's modulus of 2.5 GPa and tensile strength of 0.6 GPa. © 2005 Wiley Periodicals, Inc. *J Appl Polym Sci* 99: 802–807, 2006

**Key words:** nylon; fiber; mechanical properties; WAXS; superstructure

## INTRODUCTION

Microfibers are very valuable from the viewpoint of industrial and medical materials and are now manufactured with highly skilled techniques, such as conjugate spinning (requiring a highly complex spinneret), islands-in-a-sea fiber spinning, melt blowing, and flash spinning.

The new preparation method of microfiber that is based on an entirely different conception from the conventional one was developed by us. The new developed method was carried out by irradiating a continuous-wave carbon dioxide (CO<sub>2</sub>) laser to fibers. The developed apparatus can wind up the microfiber as a monofilament in the winding speed range of 100 to 2500 m/min<sup>-1</sup> and was already applied to poly(ethylene terephthalate) (PET)<sup>1,2</sup> nylon 6,<sup>3,4</sup> isotactic polypropylene (i-PP),<sup>5</sup> and poly(L-lactic acid)<sup>6</sup> fibers, and their microfibers were successfully prepared.

In the laser thinning, the temperature of the fiber locally heated by the CO<sub>2</sub> laser instantly reaches a high temperature that exceeds its melting temperature. The melt viscosity in the part of the fiber laser irradiated at a high power becomes sufficiently low without elongation or cutting, and the part heated by the laser enters a nearly molten state. The fiber is continuously thinned by the plastic flow occurring from the nearly molten state, and then the microfiber, having fallen down because of its own weight, is wound on the winding spool. The instantaneous plastic flow at a high strain rate induces the molecular orientation and crystallization despite a large deformation, just like in flow drawing, and gives an oriented microfiber. Thinning by use of the CO<sub>2</sub> laser may be considered a dieless spinning.

In this study, the superstructure and mechanical properties of the nylon 66 microfibers obtained under various laser-thinning conditions will be discussed in detail.

## EXPERIMENTAL

### Materials

Original nylon 66 fibers were produced from commercial grade nylon 66 pellets using a laboratory-scale

Correspondence to: A. Suzuki (a-suzuki@yamanashi.ac.jp).

Contract grant sponsor: Japan Society for the Promotion of Science.

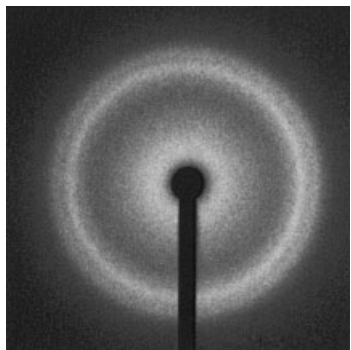


**Figure 1** Wide-angle X-ray diffraction pattern of nylon 66 original fiber.

melt extruder and take-up unit. The original fibers were spun into monofilaments at a spinning temperature of 285 °C. The original fiber had a diameter of 50 μm, degree of crystallinity of 33%, and birefringence of  $1.65 \times 10^{-3}$ . An as-spun fiber was isotropic from a wide-angle X-ray diffraction pattern, as shown in Figure 1.

### Measurements

Birefringence was measured with a polarizing microscope equipped with a Berek compensator (Olympus Optical, Tokyo, Japan).

Scanning electron microscopy (SEM) micrographs of the fibers were taken with a JSM6060LV (Tokyo, Japan) with an acceleration voltage of 5 kV.

Infrared measurements were made on a Fourier transform infrared (IR ms/SIRM) microscope (Spectratech) at a resolution of 4 cm<sup>-1</sup>. Each spectrum resulted from an accumulation of 1024 scans.

Wide angle X-ray diffraction (WAXD) images of the fibers were taken with an imaging-plate (IP) film and an IP detector R-AXIS DS3C (Rigaku, Akishima Japan). The IP film was attached to an X-ray generator (Rigaku) operated at 40 kV and 35 mA. The radiation was Ni-filtered Cu K<sub>α</sub>. The sample-to-IP film distance was 65 mm. The fibers were exposed for 30 min to the X-ray beam from a pinhole collimator with a diameter of 1.0 mm.

Differential scanning calorimetry (DSC) measurements were carried out using a Therm Plus 2 DSC 8230C calorimeter (Rigaku). The DSC scans were performed within the temperature range of 25 to 280°C, using a heating rate of 10 °C min<sup>-1</sup>. All DSC experiments were carried out under a nitrogen purge. The DSC instrument was calibrated with indium.

Young's modulus and tensile strength were measured at 23°C and a relative humidity of 50% with EZ Graph (Shimadzu). A gauge length of 20 mm and elongation rate of 10 mm min<sup>-1</sup> were used. The ex-

perimental results are the average of 10 measurements.

### Continuous-laser-thinning apparatus

The laser-thinning apparatus used to continuously produce the microfiber consisted of spools supplying and winding the fiber, a continuous-wave CO<sub>2</sub>-laser emitter (PIN10S, Onizca Glass, Oume, Japan), a system supplying the fiber, and a traverse (Fig. 2). The continuous-wave CO<sub>2</sub> laser emitted light at 10.6 μm, and the laser beam had a 4.0-mm diameter. The power density was measured with a power meter during the laser irradiation. It was necessary to supply the fiber to a laser-irradiation point at a constant speed to prepare the microfiber in a stable manner. The supplying system pulled the original fiber from the supplying spool and supplied it to the laser-irradiation point at a constant speed. The supplying system played an important role in the continuous-laser-thinning apparatus. The fiber thinned at the laser irradiating point was wound on the spool at a winding speed of 100–2500 m min<sup>-1</sup>.

### RESULTS AND DISCUSSION

The diameter of microfiber obtained by the CO<sub>2</sub> laser thinning depended on the supplying speed ( $S_s$ ) of the original fiber, the laser power density (PD), and the speed winding up the obtained microfiber. There is close relationship along the PD,  $S_s$ , and winding speed ( $S_w$ )<sup>4, 5</sup>. In the preparatory experiment, when the nylon 66 fiber, which was obtained by irradiating the laser at PD = 8.0 W cm<sup>-2</sup> to the original fiber supplied at  $S_s = 0.23$  m min<sup>-1</sup>, was wound up at speed less than 2000 m min<sup>-1</sup>, stable winding was possible without cutting the microfiber. Therefore, all irradiation was carried out at  $S_s = 0.23$  m min<sup>-1</sup> and PD = 8.0 W

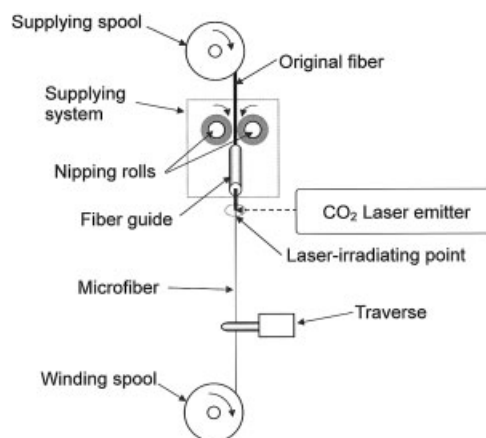


**Figure 2** CO<sub>2</sub> laser-thinning apparatus used for producing the microfiber.

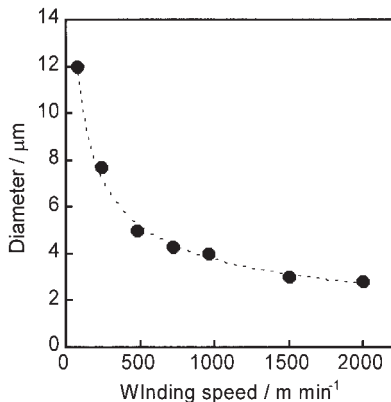


**Figure 3** Winding speed dependence of the diameter of the microfibers.

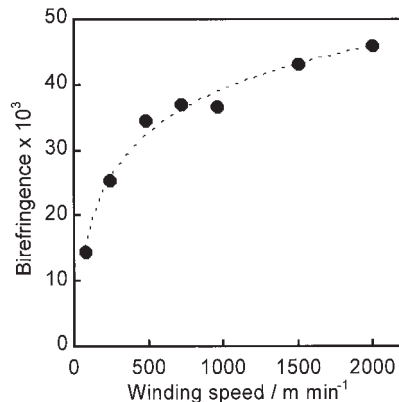


**Figure 5** Winding speed dependence of the birefringence of the microfibers.

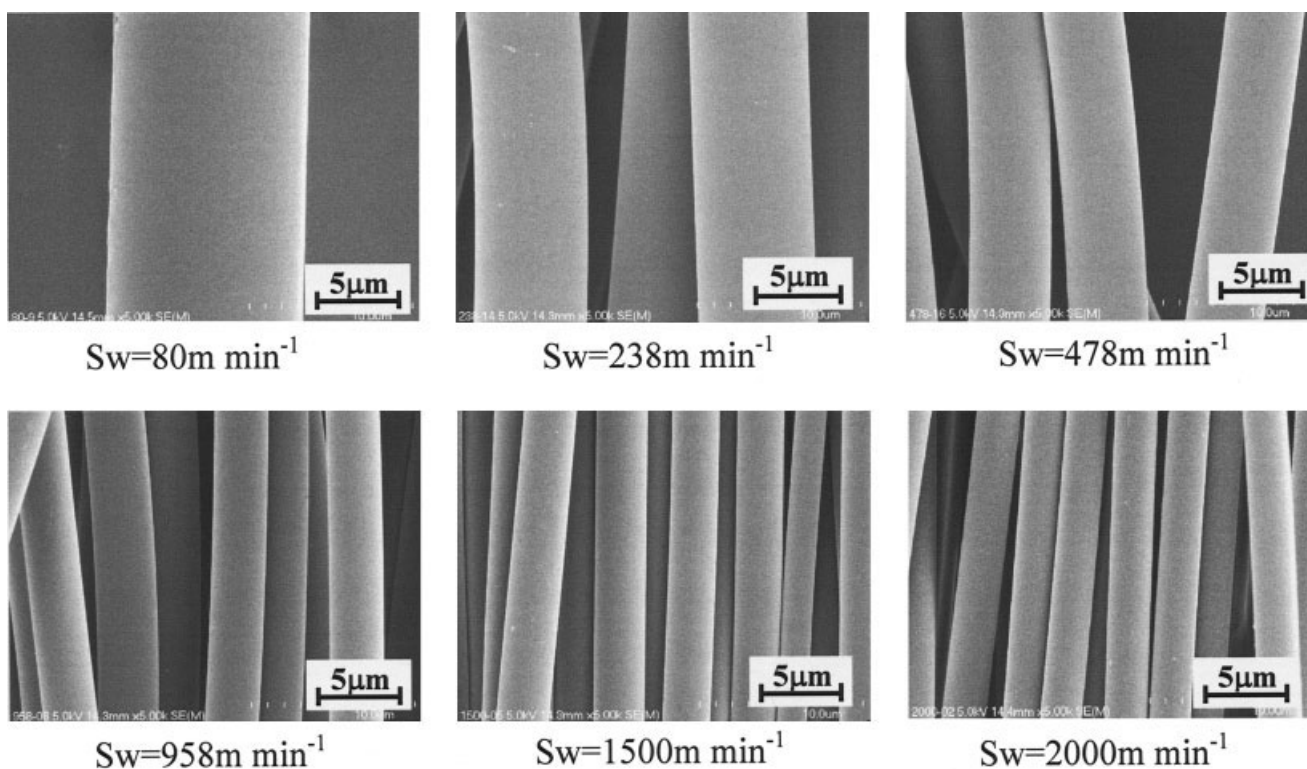
cm<sup>-2</sup>. It was difficult to continuously thin the nylon 66 fiber, except under these conditions.

Figure 3 shows the  $S_w$  dependence of the diameter of the microfibers. The diameter decreased as the  $S_w$  increased. When the microfiber was wound on the spool at 2000 m min<sup>-1</sup>, the thinnest microfiber with a diameter of 2.8 μm was obtained. Its draw ratio, estimated from the  $S_s$  and  $S_w$ , was 8696×. It has been impossible to attain such a high draw ratio with any conventional drawing.

Figure 4 shows SEM photographs of microfibers wound at six different  $S_w$ 's. SEM at 5000× showed

that these microfibers had smooth surfaces not roughened by laser ablation that were uniform in diameter.

Figure 5 shows the  $S_w$  dependence of the birefringence of the microfibers. The birefringence increased as  $S_w$  increased. The microfiber with the highest birefringence of  $46 \times 10^{-3}$  was obtained when the microfiber was wound up at  $S_w = 2000$  m min<sup>-1</sup>; its birefringence was equivalent to about 48% of the intrinsic crystallite birefringence ( $96 \times 10^{-3}$ ).<sup>7</sup> The increase in birefringence implies improvement in the orientation of amorphous molecular chain and increased degree of crystallinity because the observed birefringence is



**Figure 4** SEM photographs of 5000 magnifications for the microfibers wound up at six different winding speeds ( $S_w$ ).

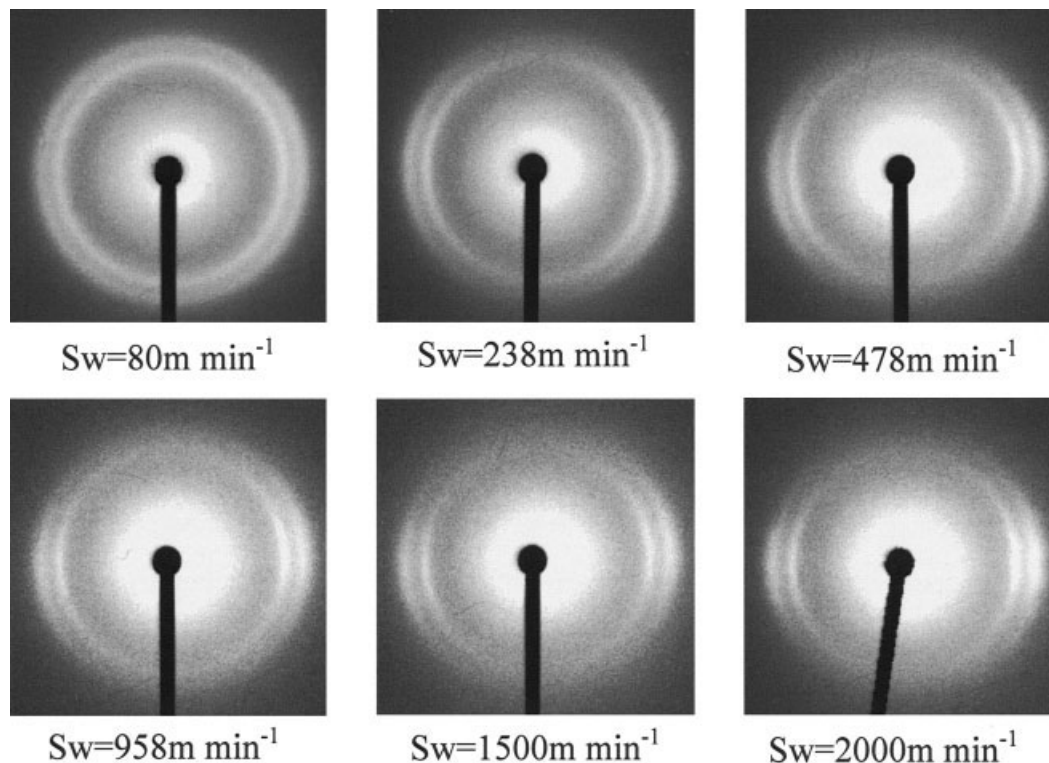


Figure 6 Wide-angle X-ray diffraction patterns of the microfibers wound up at six different winding speeds ( $S_w$ ).

the sum of crystalline and amorphous birefringence values.<sup>8</sup>

Figure 6 show WAXD patterns of microfibers wound at a series of  $S_w$ 's. The nylon 66 has two known crystal modifications: an  $\alpha$  form and a  $\beta$  form,<sup>9</sup> but no reflection due to the  $\beta$  form was observed in their WAXD patterns. The shape of the diffraction pattern due to (100) reflection and (010)/(110) doublet of the  $\alpha$  form, which were observed in the microfibers obtained at the lowest  $S_w = 80 \text{ m min}^{-1}$ , was almost the Debye ring. The diffraction pattern gradually changed into the arc-shape pattern as the  $S_w$  increased. The equatorial diffraction pattern due to the (100) reflection and (010)/(110) doublet becomes sharp with increasing  $S_w$ .

Figure 7 shows the degree of crystallite orientation estimated from the half-width of the meridional diffraction pattern due to the (010)/(110) doublet. The degree of crystal orientation increased as the  $S_w$  increased and then reached 80% at  $S_w = 2000 \text{ m min}^{-1}$ . The obtained value is slightly lower than that of the zone-annealed nylon 66 fiber.<sup>10</sup> Winding microfiber at the higher  $S_w$  induced the highly oriented crystallites, although the microfiber was obtained by the plastic flow occurring from the nearly molten state. The highly oriented crystallites formed by the flow-induced crystallization increased as the  $S_w$  increased.

Figure 8 shows the change in the intensity ratio of the *trans* band<sup>11</sup> at  $936 \text{ cm}^{-1}$  and *gauche* band<sup>11</sup> at  $1136 \text{ cm}^{-1}$  with the  $S_w$ . The former has been assigned to a

C-CO stretching and the latter to a CO twisting movement. The *trans* conformation can be involved in the crystalline and the amorphous phases, but the *gauche* conformation can be found only in the amorphous phase. The *trans/gauche* ratio slightly increased at  $S_w = 478 \text{ m min}^{-1}$  or lower as the  $S_w$  increased and then rapidly increased at the  $S_w$  of faster than  $478 \text{ m min}^{-1}$ . The change in conformation from *gauche* to *trans* taken place on the winding at the faster  $S_w$ . The increase of *trans* conformation can be attributed to the increase in

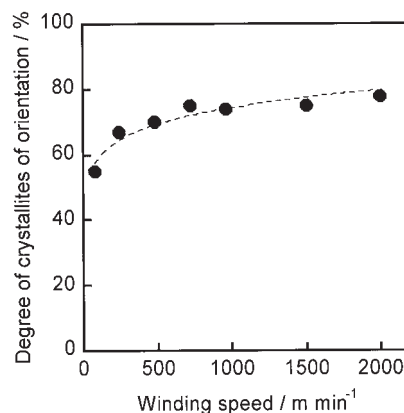
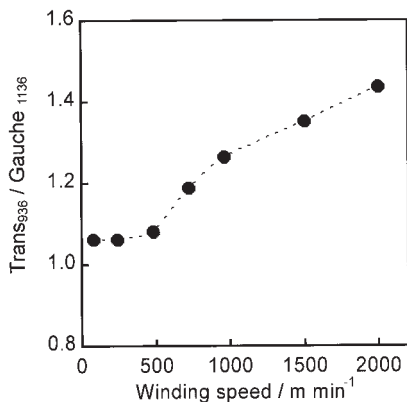


Figure 7 Winding speed dependence of degree of crystallites orientation estimated from the half-width of the meridional diffraction pattern due to the (010)/(110) doublet.



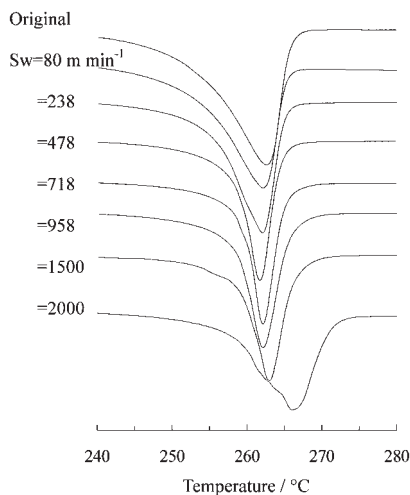


**Figure 8** Change in the intensity ratio of *trans* band at 936  $\text{cm}^{-1}$  and *gauche* band at 1136  $\text{cm}^{-1}$  with the winding speed.

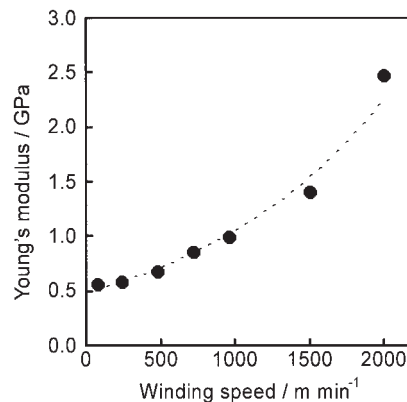
the degree of molecular orientation and the flow-induced crystallization due to the rapid plastic flow occurred from the nearly molten state. In the annealing of PET fiber, the *gauche* band decreased with annealing temperature, whereas the *trans* band increased due to conformational changes that take place on annealing.<sup>12–14</sup>

Figure 9 shows DSC curves for the original fiber and the microfibers wound up at a series of  $S_w$ 's. The original fiber shows a broad melting endotherm peaking at 262.8°C. Its melting peak can be attributed to melting of a folded chain crystal (FCC) in the original fiber and/or to the FCC of  $\alpha$  form, which recrystallized during DSC scanning<sup>15,16</sup> because the  $\alpha$  form was obtained by crystallization from the melt.<sup>7</sup>

The microfibers obtained at  $S_w$  of 958  $\text{m min}^{-1}$  or lower have melting endotherm peaking at about 262 °C. Their melting temperatures were almost the same as the original fiber, but the melting peak becomes



**Figure 9** DSC curves of the original fiber and the microfibers wound up at seven different winding speeds ( $S_w$ ).



**Figure 10** Change in Young's modulus of the microfibers with winding speed.

sharp with increasing  $S_w$ . A sharpening of the melting peak is caused by an increase in the degree of perfection of the crystallites.<sup>17,18</sup> Their melting peaks were attributable to extended chain crystallites formed by the flow-induced crystallization because the *trans* conformation increased as the  $S_w$  increased. The microfiber obtained at  $S_w = 1500 \text{ m min}^{-1}$  has the sharper single melting endotherm peak at 263.2°C. The microfiber wound up at 2000  $\text{m min}^{-1}$  has a melting endotherm peaking at 266°C and a trace of shoulder on the lower temperature side of its peak. Winding microfiber at the faster  $S_w$  induced the crystallites with a higher melting point.

Figures 10 and 11 show the changes in Young's modulus and tensile strength of the microfibers with the  $S_w$ . Because the microfibers obtained at  $S_w = 478 \text{ m min}^{-1}$  or less stretched exceeding the range of measurement, their tensile strengths was not obtained. In the  $S_w$  dependence of Young's modulus and the tensile strength, these values increased as the  $S_w$  increased. The microfiber wound on the spool at  $S_w = 2000 \text{ m min}^{-1}$  had a Young's modulus of 2.5 GPa and a tensile strength of 0.60 GPa.

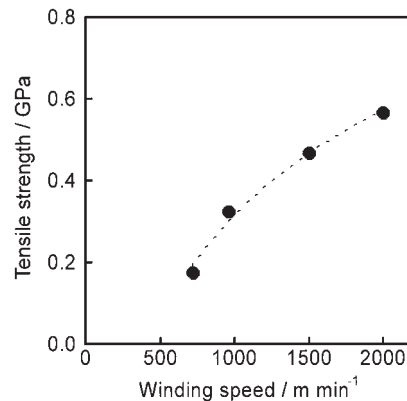


**Figure 11** Change in tensile strength of the microfibers with the winding speed.

The increase in mechanical properties was closely related to the improvement in the orientation of molecular chain and increase in the degree of the crystallization as the  $S_w$  increased. The mechanical properties of the microfiber obtained at the highest  $S_w$  were lower than those (Young's modulus: 8 GPa, tensile strength: 1.2 GPa) of the zone-drawn nylon 6 fiber.<sup>10</sup> The lower mechanical properties of the obtained microfiber were attributed to the lack of the highly oriented amorphous chains and crystallites. It is necessary to draw and anneal the microfiber obtained to improve its mechanical properties. We are going to zone-draw and zone-anneal the nylon 66 microfiber to increase its mechanical properties, because the microfiber obtained by the laser thinning can be drawn and annealed in the same manner as the zone-drawing of the PET<sup>19</sup> and i-PP<sup>20</sup> microfibers.

### CONCLUSIONS

The CO<sub>2</sub>-laser-thinning method, which could produce microfibers of various polymers, was applied to nylon 66 fibers. The diameter decreased and the birefringence increased as the winding speed increased. When microfibers, obtained by laser irradiating (at a power density of 8.0 W cm<sup>-2</sup>) the original fiber supplied at 0.23 m min<sup>-1</sup>, were wound at  $S_w = 2000$  m min<sup>-1</sup>, they had a diameter of 2.8 μm and a birefringence of  $46 \times 10^{-3}$ . The draw ratio calculated from the  $S_s$  and  $S_w$  was 8696×. The nylon 66 microfiber was

obtained by the laser thinning in the same manner as PET, nylon 6, i-PP, and poly(L-lactic acid) fibers.

### References

1. Suzuki, A.; Mochizuki, N. *J Appl Polym Sci* 2003, 88, 3279.
2. Suzuki, A.; Mochizuki, N. *J Appl Polym Sci* 2003, 90, 1955.
3. Suzuki, A.; Kamata, K. *J Appl Polym Sci* 2004, 92, 1449.
4. Suzuki, A.; Kamata, K. *J Appl Polym Sci* 2004, 92, 1454.
5. Suzuki, A.; Narisue, S. *J Appl Polym Sci* 2004, 92, 1534.
6. Suzuki, A.; Daisuke, M.; Hasegawa, T. *Polymer* 2005, 46, 5550.
7. Danford, M. D.; Spruiell, J. E.; White, J. L. *J Appl Polym Sci* 1978, 22, 3351.
8. Stain, R. S.; Norris, F. N. *J Polym Sci A Polym Chem* 2001, 82, 2775.
9. Bunn, C. W.; Garner, E. V. *Proc R Soc* 1947, A189, 39.
10. Suzuki, A.; Chen, Y.; Kunugi, T. *Polymer* 1998, 39, 5335.
11. Quintanilla, L.; Rodriguez-Cabello, J. C.; Pastor, J. M. *Polymer* 1994, 35, 2321.
12. Quintanilla, L.; Rodriguez-Cabello, J. C.; Jawhari, T.; Pastor, J. M. *Polymer* 1993, 34, 3787.
13. Boerio, F. J.; Bahl, S. K. *J Polym Sci Polym Phys Ed* 1976, 14, 1029.
14. Lin, S. B.; Köenig, J. L. *J Polym Sci Polym Phys Ed* 1983, 21, 2277.
15. Pecorini, T. J.; Hertzberg, R. W. *Polymer* 1993, 34, 5053.
16. Quintanilla, L.; Rodriguez-Cabello, J. C.; Pastor, J. M. *Polymer* 1994, 35, 2321.
17. Wills, A. J.; Capaccio, G.; Ward, I. M. *J Polym Sci Polym Phys Ed* 1980, 18, 493.
18. Gaymans, R. J.; Van Utteren, T. E. C.; Van Der Berg, J. W. A.; Schuyer, J. *J Polym Sci Polym Chem Ed* 1977, 15, 537.
19. Suzuki, A.; Okano, T. *J Appl Polym Sci* 2004, 92, 2989.
20. Suzuki, A.; Narisue, S. *J Appl Polym Sci*, to appear.